

# Improving phase Doppler volume flux measurements in low data rate applications

John F Widmann<sup>1</sup>, Cary Presser<sup>2</sup> and Stefan D Leigh<sup>3</sup>

National Institute of Standards and Technology, Gaithersburg, MD 20899-8663, USA

E-mail: john.widmann@nist.gov, cpresser@nist.gov and stefan.leigh@nist.gov

Received 20 November 2000, in final form 17 May 2001, accepted for publication 6 June 2001

## Abstract

Phase Doppler interferometry (PDI) measurements in low number density sprays necessitate a compromise between collecting a large number of samples for adequate statistics and practical data acquisition times. This paper investigates the effect of insufficient sample statistics on the calculated probe area, and the resultant uncertainty in the volume flux measurement. Several methods of improving the probe area calculation and volume flux measurement are investigated using experimental data obtained from water sprays produced by residential fire sprinklers. It is shown that the corrections result in statistically significant improvements in the volume flux measurements.

**Keywords:** droplets, fire sprinklers, phase Doppler anemometry, phase Doppler particle analyser, phase Doppler interferometry, multiphase flow, sprays, volume flux measurements

## 1. Introduction

Since its introduction [1–6], phase Doppler interferometry (PDI) has been used to characterize sprays in numerous areas including spray combustion, spray coatings, pesticide applications, fire suppression and others. PDI, which is an extension of laser Doppler velocimetry, involves creating an interference pattern in the region where two laser beams intersect. The region where the laser beams intersect is called the *sample volume* or *illumination volume*, and a droplet passing through the sample volume scatters light that exhibits an angular and temporal intensity distribution characteristic of the size, refractive index and velocity of the droplet. For a droplet with known refractive index, the size and velocity can be determined by analysing the scattered light.

Phase Doppler interferometry is a single-point (or spatially resolved) diagnostic instrument providing information about the spray at a single point in space. Only by moving the sample volume throughout the spray can one map the spatial profile of the spray characteristics. PDI is also a single-particle

technique in that information is obtained for one droplet at a time. This offers advantages over integrating techniques because the characteristics of a particular droplet (size, velocity etc) can be recorded and the data can be separated into classes (size classes, velocity classes) to further characterize the spray system. For a review of the principles and applications of PDI measurements, the reader is referred to [7].

To avoid confusion, several terms need to be defined concerning the PDI method. The *sample volume*, which was defined above, refers to the region in space where the laser beams intersect. The diameter of the sample volume is defined using some intensity decay criteria which, for laser beams with a Gaussian intensity profile, is typically defined as the location where the beam intensity falls to  $1/e^2$  of the maximum intensity. Closely related to the sample volume is the *measurement volume*, which is the same size as the sample volume but is displaced in space. The displacement of the measurement volume relative to the sample volume is determined by the scattering order utilized and the location of the detectors used to measure the light scattered by the droplets. The *probe volume* or *detection volume* is the region of space in which valid measurements can be obtained, and may be larger or smaller than the measurement volume depending upon the operating parameters used (e.g. PMT gain). The droplet

<sup>1</sup> Corresponding author. Building and Fire Research Laboratory.

<sup>2</sup> Chemical Science and Technology Laboratory.

<sup>3</sup> Information Technology Laboratory.

trajectory may also affect the dimensions of the probe volume, particularly for droplets that are large compared to the probe volume dimensions.

Numerous metrology issues related to PDI measurements have been reported. Those receiving the most attention in the literature have included the difficulty quantifying the dimensions of the probe volume (e.g. [8–14]), the effect of the PMT gain on the measurements (e.g. [15–19]), trajectory dependent scattering errors that result from the Gaussian intensity profile of the laser beams (e.g. [20–32]) and signal attenuation due to large optical path lengths (e.g. [33–36]). Note that these measurement issues are not independent. For example, the droplet size bias of the probe volume, the PMT gain and trajectory dependent scattering errors all affect the accurate determination of the probe volume, volume flux and number density.

There have been many investigations conducted in which the accuracy of PDI volume flux measurements was reported. Although accurate volume flux measurements are more difficult to obtain than size or velocity measurements, the accuracy can be evaluated either by comparison with independent measurement techniques or by comparison of the integrated volume flux profiles across a plane orthogonal to the flow direction with the liquid flow rate through the atomizer. Unfortunately, the results of these studies display considerable variability. For example, shortly after commercial phase Doppler interferometers became available, Dodge *et al* [37] compared the PDI and laser-diffraction techniques in the spray produced by a small pressure-swirl atomizer. These researchers reported integrated volume flux measurements that varied from a small percentage of the total flow through the nozzle (measured within 5 mm of the nozzle) to 500% of the total flow through the nozzle (measured 35 mm downstream of the nozzle). Subsequent studies indicate improvements in PDI volume flux measurements since that early study; however, difficulties obtaining accurate measurements in the dense region of the spray near the nozzle have continued to plague researchers (e.g. [18, 38–44]).

It was recognized early in the development of PDI that accurate measurements of size and velocity distributions, number density, and volume flux required *in situ* determination of the probe volume dimensions for a variety of reasons, including the variation in the probe volume with droplet size [8]. By determining the probe area *in situ*, Bachalo *et al* [9] reported agreement to within 10% between mass flux measurements obtained with PDI and those obtained using a sampling probe. Dodge and Schwalb [45] obtained volume flux measurements in a non-reacting spray generated with a pressure-swirl atomizer and reported good agreement between the integrated volume flux and the liquid flow through the atomizer. Several reasons were given for the improved volume flux measurements over their previous study, including improved alignment of the receiving optics, reducing the width of the slit aperture in the receiving optics, avoiding the top end of the size range, operating without frequency shifting, and optimizing the gain of the PMT detectors. McDonnell and Samuelsen [39] compared PDI volume flux measurements in reacting and non-reacting sprays. For the non-reacting case, they reported the integrated volume flux at 50 mm downstream of the atomizer to be about 60% of the flow through the

nozzle, and indicated that the agreement improved further downstream.

Lazaro [34] evaluated the feasibility of using PDI to obtain mass flux measurements in high number density sprays. He reported that the mass flux was overpredicted due to burst splitting events, in which single droplets were counted multiple times, that resulted from attenuation of the transmitting laser beams. Lazaro noted that there was a double effect on the measurements: (i) a fraction of the droplets were counted multiple times (approximately 20% in his experiments), and (ii) the experimentally determined probe area was underpredicted due to incorrectly calculated transit times. The probe area is the cross-sectional area of the probe volume in the mean flow direction. Van Den Moortel *et al* [35] presented a post-processing algorithm to account for burst splitting events, but noted that identifying burst splitting in PDI measurements was difficult due to the very small characteristic times associated with the beam coherence/intensity fluctuations that cause the effect. Widmann *et al* [36] presented several methods of identifying burst splitting events in PDI measurements, and demonstrated that the effect can be minimized by carefully selecting the sampling rate and low pass filter in the processing electronics.

Qiu and Sommerfeld [12] presented a method of calibrating the probe area dimensions to remove the particle size bias in the measurements and improve the mass flux calculations, which they called the logarithmic mean signal amplitude method. They reported integrated mass flux measurements that agreed to within 5% of the liquid flow through their spray nozzle at 15 mm downstream of the nozzle, and better agreement at planes 25 mm and 50 mm downstream of the nozzle. Despite their promising results, the logarithmic mean signal amplitude method has not been widely adopted, and has been used primarily in their laboratory (e.g. [13, 46, 47]). Bulzan *et al* [40] compared measurements and predictions of a liquid spray from an air-assist nozzle. They used a two-component PDI system and noted that the validated samples varied from 20% to 90% of the total attempts depending upon the measurement location within the spray. Measurements in locations near the centre of the spray and close to the injector exit showed the largest number of signal rejections. They reported very poor agreement between the measured (integrated) volume flux and the flow rate of liquid metered through the atomizer at 5 cm downstream of the nozzle, with the agreement improving to 35 % of the measured liquid flow rate at 20 cm downstream of the nozzle. At axial locations of 30 cm and 50 cm, the integrated volume flux measurements improved to 46% and 109% of the flow through the nozzle, respectively.

Zhu *et al* [10] obtained mass flux measurements in reacting and non-reacting swirling flows. They observed poor agreement between the integrated volume flux and the flow rate through the nozzle for swirling flows, and attributed the discrepancy to the difficulty in determining the trajectory dependent probe volume correction for 3D flows. These researchers also corrected the volume flux measurement to account for flow reversal (i.e. droplets with negative velocities were subtracted from the flux measurement), an approach which has been rarely reported in the literature. In fact, volume flux has traditionally been treated as a scalar quantity

in PDI measurements. Recently, however, one manufacturer of commercial PDI systems modified their PDI software to obtain vector volume flux measurements, accounting for droplets with negative velocities and resulting in individual vector components of the flux [48].

McDonell and Samuelsen [18] reported the results of an investigation aimed at quantifying the uncertainties in PDI measurements for various applications. They concluded that PDI permits highly accurate measurements of size and velocity of individual droplets; however, significant uncertainties exist in the construction of size and velocity distributions due to the polydisperse nature of the spray and the operation of the instrument. One noteworthy aspect of this study was the tendency for the instrument to miss droplets passing through the probe volume. Using a vibrating orifice aerosol generator [49] to generate a linear array of monodisperse droplets, the counting efficiency was measured, where the counting efficiency was defined as the ratio of the number of droplets detected to the number of droplets passing through the probe volume. McDonell and Samuelsen reported counting efficiencies varying from 37% to 77%, and noted that the measured volume flux was directly proportional to the counting efficiency. Widmann *et al* [50] observed the same measurement artifact during PDI measurements in a reacting fuel spray and developed a correction based upon a Poisson model of the droplet arrival times.

Recently, the emphasis in PDI development has been to obtain accurate measurements in applications in which the droplet diameters are of the same order or larger than the probe volume dimensions. For example, rocket fuel and diesel fuel injectors produce very dense sprays requiring small PDI probe volumes to minimize the likelihood of multiple droplets being present simultaneously in the probe volume. To avoid the errors associated with trajectory ambiguities [20–32], several approaches have been adopted. Those involving introducing additional detectors have not been adopted by manufacturers of commercial PDI systems due to the additional cost and complexity; however, two approaches that are compatible with the standard PDI arrangement have been adopted. These two easily implemented procedures are intensity validation [11, 21, 25, 28, 29, 32], in which minimum and maximum intensity limits are imposed upon the scattered signal, and a non-integer phase ratio method [28, 29, 32], in which the detector spacing is adjusted to further reduce trajectory ambiguities. Together, these two methods have been very effective in reducing the errors associated with trajectory ambiguities, and permitting much more accurate volume flux measurements in dense sprays.

The single-point nature of PDI permits measurements with high spatial resolution; however, this can also present a problem for sprays that cover large areas. For example, fire sprinklers produce water sprays covering areas of order 10 m<sup>2</sup>. Thus, characterizing such a spray using single-point diagnostic techniques can be tedious. Furthermore, the number density of the droplets is relatively low because the spray is spread over such a large area. As a result of the low droplet number density, long acquisition times are required to collect a statistically significant number of samples to accurately estimate size and velocity distributions. It is therefore necessary to compromise between collecting a large number of droplet statistics and acquiring data within a reasonable time period.

This paper presents the results of a study to explore the effect of collecting a less than optimal number of droplet statistics on the calculated probe area, and the consequent uncertainty in the volume flux measurement. Several simple methods are proposed to obtain an improved estimate of the probe area, and it is shown that the corrections result in statistically significant improvements in the volume flux measurement. Furthermore, a novel method of determining the best estimate of the probe area is presented for applications in which the volume flux can be determined independently of the PDI measurements.

## 2. Probe area and volume flux measurements

The PDI system measures the size and velocity of individual droplets as they pass through the probe volume. Size and velocity distributions can then be estimated by measuring the characteristics of a large number of droplets. Furthermore, the volumetric flow rate through the probe volume can be computed using the volume and velocity of individual droplets. The volume flux,  $F_{vol}$ , is obtained from the volumetric flow rate as

$$F_{vol} = \frac{\text{volumetric flow rate}}{\text{probe area}} = \frac{\pi N_{cor} D_{30}^3}{6 t_{acq} A_p} \quad (1)$$

Here,  $N_{cor}$  is the probe volume corrected number density,  $t_{acq}$  is the acquisition time, and  $A_p$  is the probe area. The probe area is determined from [10]

$$A_p = \frac{D(d_{max})_{max} \omega_{slit}}{\sin \theta} \quad (2)$$

where  $\omega_{slit}$  is the projected image length of the slit aperture, which limits the length of the probe volume, and  $\theta$  is the scattering angle measured from the direction of propagation of the laser beams. The diameter of the probe volume,  $D(d_{max})_{max}$ , corresponds to the effective diameter of the laser beam where the light intensity is sufficient for the largest droplets to be detected.

The volume mean diameter,  $D_{30}$ , is given by [51]

$$D_{30} = \left( \frac{\sum_{i=1}^n c_i^{cor} d_i^3}{\sum_{i=1}^n c_i^{cor}} \right)^{1/3} \quad (3)$$

where  $d_i$  is the diameter of the  $i$ th droplet size class. The probe volume corrected count,  $c_i^{cor}$ , is a correction applied to account for the dependence of the probe volume on the droplet size. This correction is also applied to the measured number density to obtain  $N_{cor}$  in equation (1).

The number density,  $N_{cor}$ , is calculated as [10]

$$N_{cor} = \frac{1}{t_{acq}} \sum_i \left( \frac{1}{V_i} \sum_j t_{trans}(i, j) \right) \quad (4)$$

where  $t_{trans}$  is the transit time of the droplets, and  $V_i$  is the effective probe volume for the  $i$ th size class. Note that the indices  $i$  and  $j$  indicate the size class and droplet occurrence, respectively. The probe volume corrected count,  $c_i^{cor}$ , is related to the effective probe volume,  $V_i$ , through the relation

$$c_i^{cor} = c_i \left( \frac{V_{max}}{V_i} \right) \left( \frac{D(d_i)_{max}}{D(d_{max})_{max}} \right) \quad (5)$$

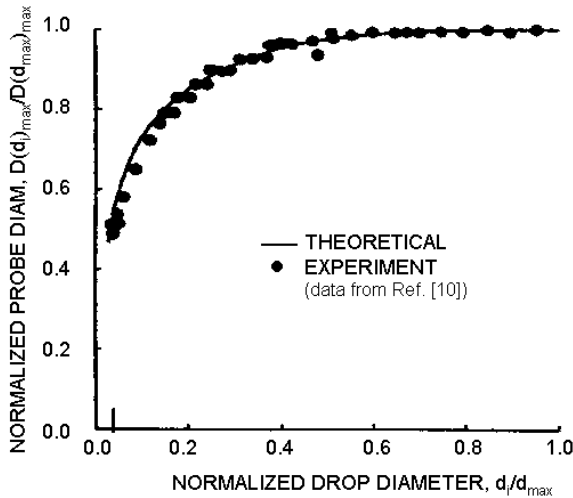


**Figure 1.** Dependence of the probe diameter on the droplet diameter. (Experimental data from [10].)

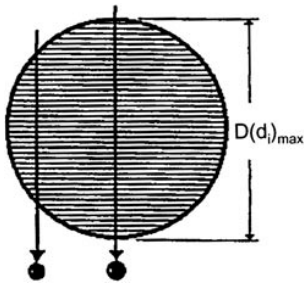


**Figure 2.** Determination of the probe diameter,  $D(d_i)_{\max}$ , by measuring the transit length through the probe volume.

where  $c_i$  is the uncorrected count in size class  $i$ , and  $V_{\max}$  is the effective probe volume for the largest size class.

To illustrate the dependence of the probe area on droplet size, the normalized probe diameter is given with respect to the normalized droplet diameter in figure 1. The droplet size dependence of the probe area results from the Gaussian intensity profile of the laser beams and the dependence of the scattered light intensity on the droplet size [9–14]. Smaller droplets must pass closer to the centre of the probe area in order to be detected by the photomultiplier tube detectors, whereas larger droplets can pass through the wings of the Gaussian profile and still scatter sufficient light to be detected. This is the reason for introducing the probe volume corrected count,  $c_i^{cor}$ , in equation (3).

The experimental data presented in figure 1 [10] were obtained by measuring the number of fringes crossed as droplets passed through the probe volume and assuming that the product of the maximum number of fringes crossed and the fringe spacing in each size class corresponds to the probe diameter for that size class. This is illustrated in figure 2. The maximum length,  $D(d_i)_{\max}$ , corresponds to the maximum number of fringes crossed multiplied by the fringe spacing. It should be noted that using this procedure implies that the longest probe diameter measured corresponds to a droplet passing directly through the centre of the probe volume, and therefore may lead to errors if an insufficient number of droplets are sampled. Recent variations of the PDI system

use the transit time of the droplets and the droplet velocity to determine the probe length, but it is still assumed that the longest probe diameter measured corresponds to the centre of the probe volume. The theoretical curve in figure 1 is a least-squares fit to the experimental data, and corresponds to a two-parameter model that accounts for the Gaussian intensity distribution of the laser beam and the droplet size dependence of the scattered light intensity [8, 10].

Using the curve in figure 1, the probe volume correction (PVC) can be computed as

$$PVC = \frac{c_i^{cor}}{c_i} = \frac{D(d_{\max})_{\max}}{D(d_i)_{\max}}. \quad (6)$$

The probe volume correction is applied to size distributions, velocity distributions, volume flux measurements, number density measurements and characteristic sizes (e.g. arithmetic mean diameter, volume mean diameter etc). Although the correction in equation (6) is called the probe *volume* correction, it is actually a correction applied to  $c_i$  due to the size dependence of the probe *area*. This is because PDI is a flux-based (temporal) measurement as opposed to a volume-based (spatial) measurement [10].

The form of the PVC defined in equation (6) will be affected by the intensity validation scheme frequently used to minimize trajectory dependent scattering errors (e.g. [28, 29, 32]). The effect of the intensity validation, which involves imposing maximum and minimum light scattering intensities for each particle size class, is to reduce the diameter of the probe volume for the larger droplets. In this study the probe volume diameter curve presented in figure 1 will show less variation due to the intensity validation scheme; however this will not impact the conclusions presented herein. The PVC may be considered to be a relative measure of the probe area in that the probe area for each size class is normalized by the maximum probe area measured, which corresponds to the largest droplet size class.

The PVC affects the calculation of the volume flux through the probe volume corrected volume mean diameter,  $D_{30}$ , and number density,  $N_{cor}$ . The procedures presented here provide improved calculations of the probe area,  $A_p$ , which corresponds to the measurement area available for the largest droplets. While the PVC affects the calculated volume flux through  $D_{30}$  and  $N_{cor}$ , it is a much weaker effect than that of  $A_p$ . In fact, the PVC has the greatest effect on the smallest size classes in the size distribution, whereas the volume flux is dominated by the larger droplets present. Furthermore, the effect of the PVC on the volume flux calculation is further reduced when intensity validation is used because the scaling due to the PVC is limited to the smallest size classes [11, 28, 29, 32]. Thus, the focus of this study is on improving volume flux measurements, and the techniques presented are not intended to improve size distribution measurements. In this study, the PVC computed by the PDI software is not modified, and attention is focused on the accurate determination of  $A_p$ .

There are several factors that contribute to errors in the calculation of the probe area. The dependence on droplet size discussed above is one factor. Second, if the droplets have a non-negligible velocity component in the direction of propagation of the laser beams, the computed probe area (using a one- or two-component system) will have an error [51].

Third, the calculated probe area may be in error due to the probe length ambiguity that results from the receiver slit blur. This has been discussed in detail by Bachalo *et al* [9]. Finally, additional uncertainties will be introduced into the probe area calculation if an insufficient number of droplets are sampled in each size class because the largest probe diameter measured may not correspond to a droplet passing through the centre of the probe area. It is the uncertainty introduced due to insufficient droplet statistics that is addressed in this paper.

### 3. Experimental results and discussion

#### 3.1. Experimental apparatus

The techniques presented here are illustrated using PDI data obtained in a water spray produced by a residential fire sprinkler. The experimental facility, presented in figure 3, has been constructed in the Building and Fire Research Laboratory at NIST for the purpose of characterizing fire sprinklers and water mist suppression systems. It consists of an enclosed area equipped with the necessary piping and pumps to operate under a variety of flow conditions. The water is collected and recirculated back to the sprinkler, forming a closed loop system. The total dimensions of the enclosed pool used to collect the water spray is 6 m × 6 m, and the sprinkler can be mounted at one of several ports 1.6 m above the floor.

The measurements were obtained in the spray produced by a residential fire sprinkler with a  $K$ -factor [52] of  $1.35 \times 10^{-4} \text{ m}^3 \text{ s}^{-1} \text{ kPa}^{-0.5}$  ( $5.6 \text{ gal min}^{-1} \text{ psig}^{-0.5}$ ). The pressure at the sprinkler head was maintained at  $131.0 \text{ kPa} \pm 6.9 \text{ kPa}$  ( $19 \text{ psig} \pm 1 \text{ psig}$ )<sup>4</sup>, resulting in a flow rate through the sprinkler of  $1.54 \times 10^{-3} \text{ m}^3 \text{ s}^{-1} \pm 0.051 \times 10^{-3} \text{ m}^3 \text{ s}^{-1}$  ( $24.4 \text{ gpm} \pm 0.8 \text{ gpm}$ ). The sprays produced by fire sprinklers are large compared to systems in which PDI is typically applied, and cover an area on the order of  $10 \text{ m}^2$ . Due to the large coverage area, it is necessary to locate the PDI transmitting and receiving optics directly in the spray. This was accomplished by encasing both the transmitting and receiving optical systems in water-tight containers equipped with a purge of dry air to prevent moisture from condensing on the optics. The PDI optics are mounted on a rectangular translation stage that can be moved in either horizontal direction. The measurements were obtained in a horizontal plane  $1.12 \text{ m} \pm 0.01 \text{ m}$  below the sprinkler. Additional details of the experimental apparatus are available elsewhere [54, 55].

Characterizing fire sprinklers using PDI is complicated by the low droplet number densities and large area covered by the spray. However, one advantage of this system is that volume flux measurements can be easily compared to an independent measurement. Pan test measurements, in which the volume flux is measured by collecting water droplets in a graduated cylinder over a known time period, can be used to assess the accuracy of the PDI flux measurements. Note that although the measurement area for the pan tests ( $31.4 \text{ cm}^2 \pm 1.0 \text{ cm}^2$ ) is considerably larger than that of the PDI (of order  $0.01 \text{ cm}^2$ ), it is orders of magnitude smaller than the area of the spray (approximately  $10 \text{ m}^2$ ). Because the characteristics of the spray do not vary significantly over the dimensions of the pan

**Table 1.** Details of the PDI optical system.

Optical parameter (channel 1)	Value
Laser wavelength (nm)	514.5
Transmitter focal length (mm)	1000
Receiver focal length (mm)	1000
Beam separation (mm)	19.96
$1/e^2$ beam waist diameter ( $\mu\text{m}$ )	655
Scattering angle ( $^\circ$ )	33
Slit aperture width ( $\mu\text{m}$ )	152
Receiver lens $f$ No	6.6
Fringe spacing ( $\mu\text{m}$ )	25.78
Detector separation AB (mm)	34.8
Detector separation AC (mm)	101

test measurement area, the fluxes determined from the pan tests can be compared directly with those obtained from the PDI measurements [54].

The phase Doppler interferometry measurements were obtained using a two-component phase Doppler particle analyser available commercially from TSI Incorporated<sup>5</sup>. The transmitting and receiving optics are fibre optically coupled to the laser beam conditioning optics and the photomultiplier tube detectors, respectively, permitting them to be positioned in the spray. The signals from the photomultiplier tubes were processed using a real-time signal analyser (RSA) processor. The front lens on the transmitting optics had a focal length of 1000 mm, and a 50 mm extender (set of collimating lenses to change the beam separation distance) was used. The receiving optics were located at a scattering angle of  $33^\circ \pm 1^\circ$  measured from the direction of propagation of the laser beams. The relatively long focal lengths of the front lenses on the receiving and transmitting optics necessitate a relatively large translation stage, and limit how close the probe volume can be located to the walls of the enclosed area. An intensity validation scheme, in which a minimum and maximum signal intensity were imposed for each size class, was used to eliminate errors due to trajectory dependent scattering effects. The details of the optical system are summarized in table 1.

Initially, burst splitting [34–36] due to droplets momentarily obscuring one of the laser beams complicated the measurements; however, this was overcome by reducing the sample rate and low pass filter setting, which minimized the impact of such burst splitting events on the measurements. The signal processor was initially operated with the settings recommended by the manufacturer for the flow investigated. The recommended operating conditions for the droplet velocities under investigation here correspond to a sample frequency of 40 MHz (the rate at which the Doppler signal is sampled), mixer frequency of 36 MHz (mixers are used to reduce the signal frequency prior to analogue-to-digital conversion) and a low pass filter setting of 20 MHz (low pass filters are used to remove the summed components from the downmixed signal, so that only the difference is used). The settings result from optimizing the processor for the expected Doppler frequency which is governed by the droplet

<sup>4</sup> Unless otherwise stated, the uncertainties expressed herein correspond to the combined standard uncertainty with a coverage factor,  $k = 2$  [53].

<sup>5</sup> Certain commercial equipment, materials or software are identified in this manuscript to specify adequately the experimental procedure. Such identification does not imply recommendation or endorsement by the National Institute of Standards and Technology, nor does it imply that the materials or equipment are necessarily the best available for this purpose.

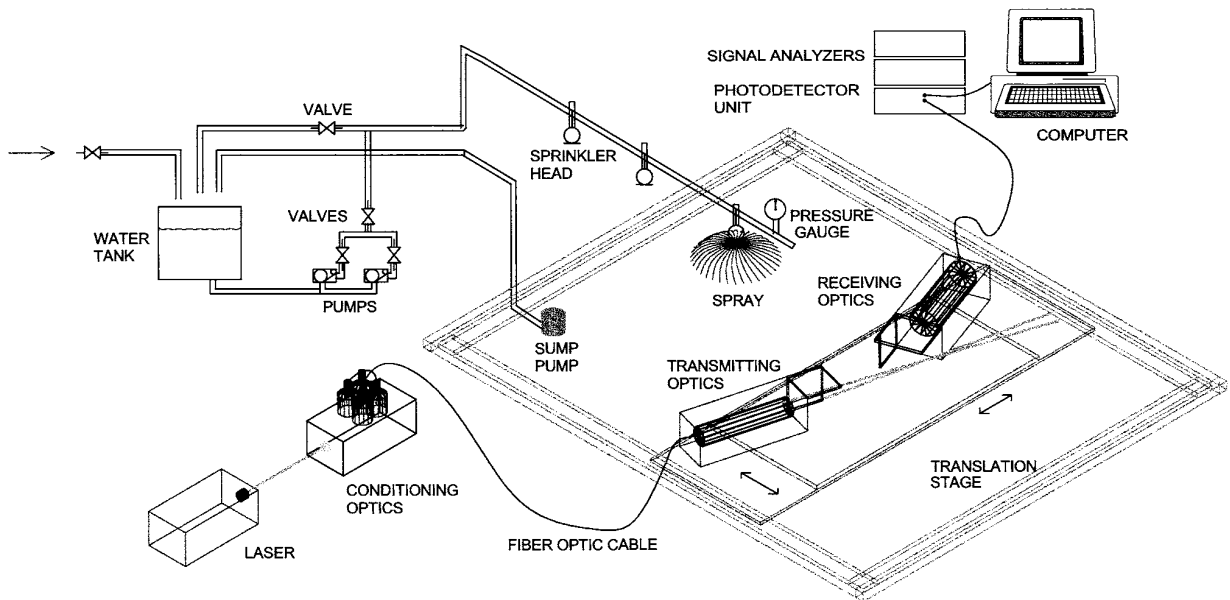


Figure 3. Schematic diagram of the experimental facility.

velocity and fringe spacing. To minimize the occurrence of burst splitting events, the processor was operated with the following parameters: mixer frequency = 40 MHz, sample frequency = 10 MHz and low pass filter = 1.25 MHz. Burst splitting events, which result in single droplets being counted as multiple droplets, have been previously reported for counter-based processors [34] and DSA frequency-based processors [35]. Our data indicate that burst splitting occurs with the RSA processors as well, but the effect on the measurements can be minimized by carefully choosing the parameters of the processing electronics. A thorough investigation of burst splitting has been conducted and the results are reported elsewhere [36].

### 3.2. Volume flux and probe area measurements

To investigate the accuracy of the volume flux measurements, 74 sample runs were collected at 15 random locations in the water spray. A sample run consisted of 2000 attempted droplet measurements. This is the maximum number of droplets that is practical due to the low data rates, which typically varied from 0.1 Hz to 10 Hz depending upon the measurement location within the spray. Because not all attempts result in valid measurements, the actual droplet count was less than the 2000 attempts. Furthermore, the data were restricted to coincident measurements which requires that the droplets be detected on both PDI channels simultaneously. All of the data were obtained under the same system configuration (e.g. laser power, PMT voltage, sampling frequency etc).

Figure 4 compares the volume flux measurements obtained with the PDI system and the pan test measurements for the 15 measurement locations. The vertical error bars (PDI measurement) in the figure correspond to the standard error of the mean. The combined standard uncertainty [53] in the pan test measurements is 6.6%, and this is shown as the horizontal error bars in figure 4. The data indicate good agreement between the PDI volume flux

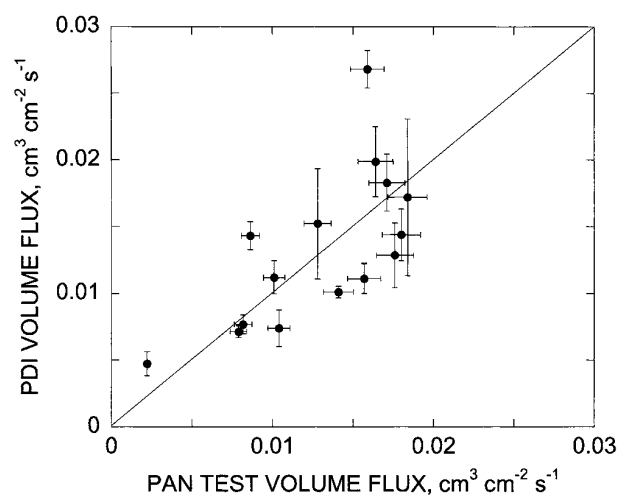
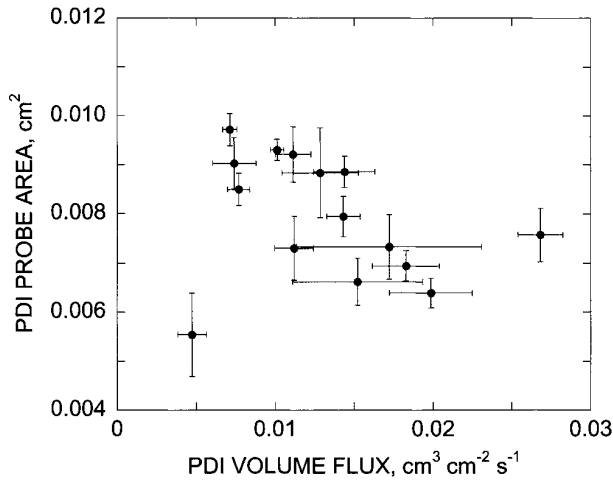


Figure 4. Comparison of PDI reported volume flux measurements and pan test measurements.

measurements and the pan tests. The mean absolute value of the relative error in the PDI volume flux measurements is  $|E| = 38.2\% \pm 4.5\%$ . Here,  $E$  is the difference between the PDI volume flux measurement and the corresponding pan test measurement at the same location, normalized by the pan test volume flux measurement. The absolute value of the error,  $|E|$ , was used to avoid positive and negative errors cancelling. It should be noted that the flux measurements obtained using PDI were significantly higher than the pan test measurements prior to eliminating the burst splitting events [36].

Reliable volume flux measurements depend directly upon the accuracy to which the probe area can be calculated [9]. This dependence is shown explicitly in equation (1). Furthermore, the calculation of the probe area is the primary source of error in the calculation of the volume flux [9–11, 45]. As shown in equation (1), the volume flux also depends upon the number density and volume mean diameter. However,



**Figure 5.** PDI probe area as a function of the reported volume flux.

as discussed above, the probe area affects  $N_{cor}$  and  $D_{30}$  only through the probe volume correction; thus, these parameters have a much weaker effect upon the volume flux than does the probe area. The objective of this paper is to present easily implemented techniques to improve the volume flux measurement by improving the probe area calculation.

The probe area in equation (1) corresponds to the largest size class for each sample run, and this is presented as a function of the PDI volume flux in figure 5. Here the error bars (vertical and horizontal) correspond to standard errors of the means [53]. The reported probe area varies significantly, ranging from approximately 0.005 cm<sup>2</sup> to 0.010 cm<sup>2</sup>. Note that all of the PDI data presented in figure 5 were obtained with the same system parameters (e.g. laser power, PMT voltage, sample rate etc), and therefore the probe area should be constant for all 15 measurement locations. This is because even if large droplets do not pass through the centre of the probe area during a specific measurement, the same total measurement area is still available. Furthermore, the probe area is a weak function of droplet size for the larger size classes, as shown in figure 1, and the variation of the probe area with droplet size is reduced further when intensity validation is utilized. This is also shown in figure 6, which presents the PDI probe area as a function of the volume mean diameter,  $D_{30}$ . Thus, the probe area should not vary significantly for different positions in the spray.

The obvious negative correlation between the volume flux and the probe area in figure 5 suggests that the volume flux measurement is significantly affected by the variation in the calculated probe area (see equation (1)). This is consistent with previous reports that the probe area calculation is the dominant source of uncertainty in the volume flux measurement [9–11, 45]. Furthermore, equation (1) suggests that multiplying the measured volume flux by the ratio of the probe area calculated *in situ* by the PDI software (from equation (2)) and a corrected probe area (to be determined) should result in improved volume flux calculations. Thus, applying the equation

$$F_{vol}^{cor} = F_{vol} \frac{A_p}{A_p^{cor}} \quad (7)$$

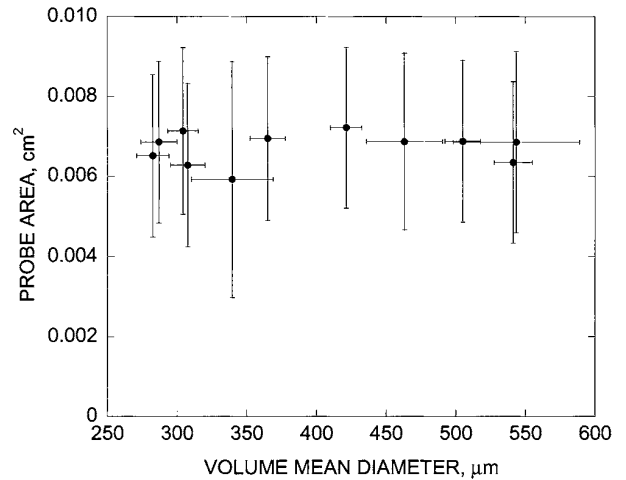


**Figure 6.** The PDI probe area as a function of the measured volume mean diameter,  $D_{30}$ .

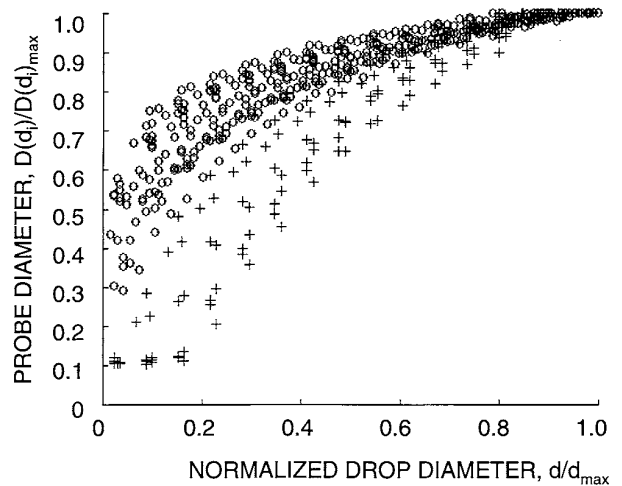


**Figure 7.** Experimental determination of the probe diameter as a function of droplet size. The symbols correspond to the accepted (○) and omitted (+) sample sets in correction method 2.

where  $F_{vol}^{cor}$  is the corrected volume flux and  $A_p^{cor}$  is the corrected probe area, should result in improved volume flux measurements.

### 3.3. Volume flux correction

As a first attempt at obtaining an improved estimate of the probe area, the mean value was calculated from the data presented in figure 5. The mean probe area for the 74 sample runs is  $A_p^{cor} = 0.00757 \text{ cm}^2 \pm 0.00016 \text{ cm}^2$ , which results in a mean relative error in the volume flux measurements of  $|E| = 26.2\% \pm 2.9\%$  following application of equation (7). This represents a reduction of 31% in the mean error in the volume flux measurement, which is a significant improvement considering the minimal effort required to apply equation (7). Estimating the true probe area as the mean of the individual probe areas as was done here will be referred to as ‘method 1’ to avoid confusion with the methods presented below.

To investigate whether the error in the volume flux measurements can be reduced further, the probe diameter

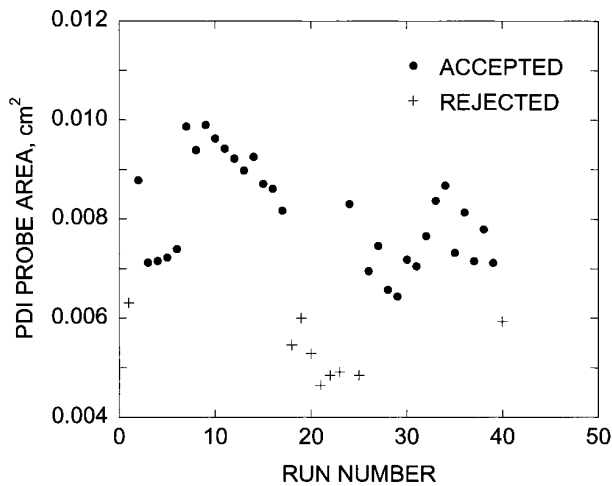


**Figure 8.** Reported PDI probe areas corresponding to the data presented in figure 7.

calculated *in situ* by the PDI software was compared with the theoretical curve in figure 1. Figure 7 shows the experimental probe diameter as a function of droplet size for 40 of the sample runs. These curves contain much more variability than the experimental data of [10] presented in figure 1. The curves in figure 7 were obtained from data sets containing significantly fewer droplets than shown in figure 1 due to the low droplet number density in the fire sprinkler spray. It is impractical to obtain a large number of samples at each measurement location due to the long acquisition times associated with low number density sprays. It is the large variation in figure 7, and the associated uncertainty in the volume flux measurement, that motivates the current investigation.

The large variability in figure 7 indicates that the calculated probe area contains errors due to insufficient droplet statistics. The second method of correcting the volume flux measurements ('method 2') involves removing those curves in figure 7 that appear to be outliers. Therefore, the curves that are depicted by the '+' symbols were omitted from the calculations (with the demarcation chosen arbitrarily—curves were omitted if the normalized probe diameter fell below 0.25 for low values of the normalized droplet diameter), and the average probe area was computed from the remaining data sets. Figure 8 presents the reported probe areas corresponding to the sample runs that were accepted and those that were rejected (outliers) based upon the visual inspection of the probe diameter versus droplet diameter curves in figure 7. There is an obvious correlation between the outliers in figure 7 and the low values of the calculated probe area. The mean value of the probe area using only the accepted sample runs is  $0.00806 \text{ cm}^2 \pm 0.00014 \text{ cm}^2$ , and the mean of the rejected probe areas is  $0.00579 \text{ cm}^2 \pm 0.00017 \text{ cm}^2$ . Applying equation (7) results in a mean relative error in the volume flux measurements of  $|E| = 24.9\% \pm 2.4\%$ , compared with  $|E| = 38.2\% \pm 4.5\%$  for the uncorrected flux measurements. This represents a 35% reduction in the mean measurement error. Note that the outliers in figure 8 that were not included in the calculation of the probe area have been included in the determination of the mean relative error in the volume flux measurements. Thus, it is not suggested that these data sets should be discarded, but rather that they should not be included

in the calculation of the probe area. It may be tempting to use the uppermost curve in figure 7 as the true probe diameter versus size class curve; however, this is not recommended because the probe area can also be over-predicted by erroneous transit time measurements [34–36].

The choice of the outliers in figure 7 is subjective, although the correlation with the low probe area measurements in figure 8 does provide some confidence that those data sets eliminated were the correct choice. To provide a more objective method of discrimination, the corrected probe area was determined from the mean of the probe areas that fall within one standard deviation of the mean of the entire data set. This eliminates probe areas at both the high and low end, compared with the previous method in which only low probe areas were rejected. Using this third method ('method 3'), the mean probe area was calculated to be  $A_p^{cor} = 0.00744 \text{ cm}^2 \pm 0.00011 \text{ cm}^2$ , which results in a mean error in the volume flux measurements of  $0.00312 \text{ cm}^3 \text{ cm}^{-2} \text{ s}^{-1} \pm 0.00041 \text{ cm}^3 \text{ cm}^{-2} \text{ s}^{-1}$  or a mean relative error of  $26.8\% \pm 3.1\%$ . The mean probe areas of the rejected sample runs were  $0.00547 \text{ cm}^2 \pm 0.00018 \text{ cm}^2$  and  $0.00937 \text{ cm}^2 \pm 0.00007 \text{ cm}^2$  for those probe areas above and below one standard deviation from the mean, respectively.

The three simple methods presented above for correcting the volume flux measurements based upon equation (7) all resulted in statistically significant improvements in the volume flux measurement. The mean corrected measurement error ranged from 24.9% to 26.8%, compared with the uncorrected mean error of 38.2%, and all three of the correction methods can be applied without knowledge of the actual flux. Furthermore, the three methods resulted in approximately equal improvement in accuracy when one considers the uncertainty in the calculations.

The corrections presented above result in improved estimates of the probe area because the data from many runs (obtained at various locations in the spray) were combined. There is one possible pitfall that must be explored when using this technique, and that is if the largest droplets measured in different locations of the spray have *significantly* different sizes. This was discussed above in connection with figure 6. The errors that might be introduced would result from the way in which the probe volume correction is applied (see equation (6)). The correction scales the probe volume corrected count,  $c_i^{cor}$ , to the maximum probe area measured. If the maximum droplet size varies significantly throughout the spray, then the correction method should only be applied to those data sets where the maximum droplet sizes are similar. By significantly different, it is implied that the largest droplets will have sizes that differ by at least a factor of two. Figure 1 indicates that variations in the maximum droplet size of a factor of two would lead to small errors in the calculated probe area (compare the normalized probe area for normalized droplet diameters of 0.5 and 1.0). Recall that intensity validation limits the diameter of the probe volume for the larger size classes, and therefore errors introduced due to varying size distributions with location within the spray are significantly reduced when intensity validation is utilized.

This potential pitfall can be identified by determining whether the reported probe areas correlate strongly with the maximum occupied size bins. Figure 9 presents the maximum

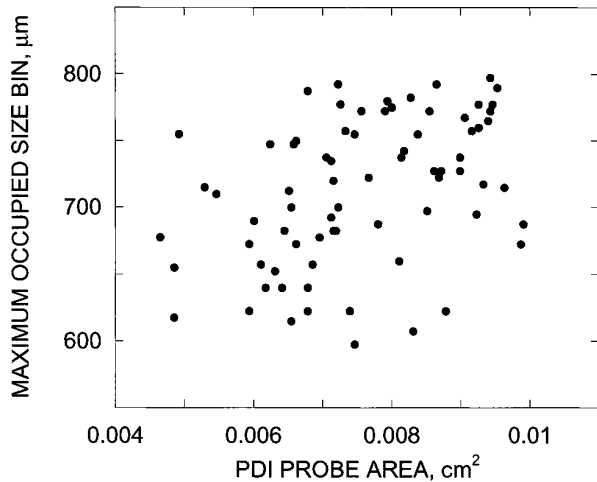


**Figure 9.** Maximum size bin containing droplet occurrences as a function of the reported probe area.

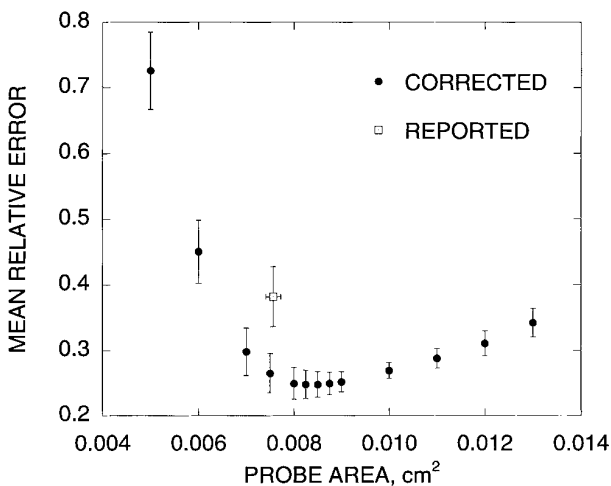


**Figure 10.** Mean relative error in the corrected PDI volume flux measurements using equation (7) for various values of the corrected probe area.

occupied size bin as a function of the reported probe area for the 74 sample runs used in this study. The correlation coefficient for this data set is  $0.407 \pm 0.095$ , which is a very weak correlation. Therefore, the techniques presented can be applied to this data set with confidence. Note that the probe volume correction has the greatest impact on the number of smaller droplets in the distribution, whereas the volume flux is dominated by the contribution from the larger droplets. Furthermore, the use of intensity validation to reduce trajectory ambiguities further reduces the effect of the PVC on volume flux measurements, as discussed above. Therefore, spatial variations in the PVC are not likely to significantly affect the computed volume flux. Note that if a strong correlation existed between the probe area calculated from equation (2) and the maximum size class, the techniques presented here could still be applied to data sets with similar maximum size classes or data sets obtained at the same location in the spray. Furthermore, these techniques can be easily implemented into PDI software.

**Table 2.** Calculated probe areas and relative errors in the volume flux measurements. The various correction methods are discussed in the text.

Correction method	Relative flux error (%)	Probe area (cm <sup>2</sup> )
Method 1	$26.2 \pm 2.9$	$0.00757 \pm 0.00016$
Method 2	$24.9 \pm 2.4$	$0.00806 \pm 0.00014$
Method 3	$26.8 \pm 3.1$	$0.00744 \pm 0.00011$
Flux known	$24.8 \pm 1.9$	$0.0085 \pm 0.0010$
No correction	$38.2 \pm 4.5$	0.005 to 0.010

### 3.4. Probe area determination

In the present study, an improved estimate of the probe area can be determined because an independent measure of the volume flux is available. Figure 10 presents the mean relative error,  $|E|$ , in the corrected volume flux measurement obtained from equation (7) for arbitrary values of the corrected probe area. Note that the three correction methods presented above provide methods of estimating  $A_p^{cor}$ , whereas the curve presented in figure 10 was calculated from equation (7) with  $A_p^{cor}$  as the independent variable. The value of the mean relative error of the uncorrected measurements is also presented for comparison. The best estimate of the probe area corresponds to the minimum in the curve. Furthermore, the envelope of the error bars provides a method of estimating the uncertainty in the calculated probe area.

The minimum mean relative error in figure 10 is  $|E|_{min} = 24.8\% \pm 1.9\%$ , which corresponds to a probe area of  $0.0085 \text{ cm}^2$ . This value of the relative error in the flux measurement represents the minimum flux error that can be obtained from this data set using the correction method of equation (7). Note that the relative error in the volume flux calculated by eliminating the outliers from the probe diameter versus droplet diameter curves (method 2) results in essentially the same value,  $24.9\% \pm 2.4\%$ . In fact, all of the methods presented result in volume flux improvements that agree with that obtained from figure 10 within the uncertainties reported.

Using the envelope of the uncertainty bars in figure 10 to obtain an estimate of the interval such that the minimum in the curve is certain to lie within this interval, the uncertainty in the probe area can be estimated. Based upon the envelope of the uncertainty bars in figure 10, the minimum in the curve is certain to lie within the interval  $[0.007, 0.0105] \text{ cm}^2$ . Assuming an equal probability of the true value to lie anywhere within this interval (uniform probability distribution), then the best estimate of the uncertainty in the probe area is  $0.0010 \text{ cm}^2$  [39]. Therefore, an improved estimate of the actual probe area for the measurements, based upon the curve presented in figure 10, is  $0.0085 \text{ cm}^2 \pm 0.0010 \text{ cm}^2$ .

Table 2 summarizes the results obtained using the three correction methods, the result obtained when the pan test measurements were used and the uncorrected measurements. The method discussed in section 3.4 is labelled ‘flux known’ because the pan test results were used to obtain the value of the corrected probe area.

## 4. Conclusion

Three methods of improving the accuracy of volume flux measurements obtained with phase Doppler interferometry have been presented, and are found to produce comparable

results. The correction methods are particularly beneficial in applications in which low data rates make it impractical to sample large numbers of droplets at each location. By averaging the probe areas computed over many data sets collected *using the same system parameters*, the probe area can be calculated with increased accuracy. These techniques can be easily incorporated into software systems by PDI system manufacturers, or applied as a post-processing algorithm by PDI users. Furthermore, the methods presented can be applied to individual locations, data sets with similar maximum droplet sizes or throughout the entire spray, depending upon the application. A method of determining the best estimate of the probe area, and a corresponding uncertainty in the estimate, has been presented for applications in which the volume flux can be determined independently of the PDI measurement.

## References

- [1] Farmer W M 1972 Measurement of particle size, number density and velocity using a laser interferometer *Appl. Opt.* **11** 2603–12
- [2] Durst F and Zare M 1975 Laser Doppler measurements in two-phase flows *Proc. LDA Symp. (Copenhagen)* pp 403–29
- [3] Durst F 1982 Combined measurements of particle velocities, size distributions and concentration *ASME J. Fluids Eng.* **104** 284–96
- [4] Bachalo W D and Houser M J 1984 Development of the phase/Doppler spray analyser for liquid droplet size and velocity characterizations *AIAA/SAE/ASME 20th Joint Propulsion Conf.*
- [5] Saffman M, Buchhave P and Tanger H 1984 Simultaneous measurements of size, concentration and velocity of spherical particles by a laser Doppler method *Proc. 2nd Int. Symp. on Applications of Laser Anemometry to Fluid Mechanics (Lisbon, 1984)*
- [6] Bachalo W D and Houser M J 1984 Phase/Doppler spray analyser for simultaneous measurements of droplet size and velocity distributions *Opt. Eng.* **23** 583–90
- [7] Bachalo W D 1994 Experimental methods in multiphase flows *Int. J. Multiphase Flow* **20** 261–95
- [8] Saffman M 1987 Automatic calibration of LDA measurement volume size *Appl. Opt.* **26** 2592–7
- [9] Bachalo W D, Rudoff R C and Brena de la Rosa A 1988 Mass flux measurements of a high number density spray system using the phase Doppler particle analyser *AIAA 26th Aerospace Sciences Meeting (Reno, NV)* paper AIAA-88-0236
- [10] Zhu J Y, Rudoff R C, Bachalo E J and Bachalo W D 1993 Number density and mass flux measurements using the phase Doppler particle analyser in reacting and non-reacting swirling flows *AIAA 31st Aerospace Sciences Meeting Exhibit. (Reno, NV)* paper AIAA-93-0361
- [11] Strakey P A, Talley D G, Sankar S V and Bachalo W D 1998 The use of small probe volumes with phase Doppler interferometry *ILASS-Americas 1998 (Sacramento, CA)* pp 286–90
- [12] Qiu H H and Sommerfeld M 1992 A reliable method for determining the measurement volume size and particle mass fluxes using phase Doppler anemometry *Exp. Fluids* **13** 393–404
- [13] Sommerfeld M and Qiu H H 1995 Particle concentration measurements by phase Doppler anemometry in complex dispersed two-phase flows *Exp. Fluids* **18** 187–98
- [14] Schöne F, Bauckhage K and Wriedt T Size of the detection area of a phase Doppler anemometer for reflecting and refracting particles *Particle Particle Syst. Characterization* **11** 327–38
- [15] Chao J, Hwang K and Lee T 1990 Sensitivity of user parameter settings of phase Doppler particle analyser in combustionspray *AIAA 21st Fluid Dynamics, Plasma Dynamics and Lasers Conf. (Seattle, WA)* paper AIAA-90-1553
- [16] McDonell V G and Samuelsen G S 1990 Sensitivity assessment of a phase Doppler interferometer to user-controlled settings *Liquid Particle Size Measurement Techniques* vol 2, ed E D Hirleman, W D Bachalo and P G Felton ASTM STP 1083 (Philadelphia, PA) pp 170–89
- [17] Presser C, Gupta A K, Avedisian C T and Semerjian H G 1994 Effect of dodecanol content on the combustion of methanol spray flames *Atomization Sprays* **4** 207–22
- [18] McDonell V G and Samuelsen G S 1995 Intra- and interlaboratory experiments to assess performance of phase Doppler interferometry *Recent Advances in Spray Combustion: Spray Atomization and Drop Burning Phenomena* vol 1, ed K K Kuo (Reston, VA: American Institute of Aeronautics and Astronautics) pp 57–106
- [19] Mao C P 1996 Measurements of sprays using phase Doppler instruments: a study to establish formal operating procedures *9th Ann. Conf. on Liquid Atomization and Spray Systems (San Francisco, CA)* pp 22–6
- [20] Sankar S V and Bachalo W D 1991 Response characteristics of the phase-Doppler particle analyser for sizing spherical particles larger than the wavelength *Appl. Opt.* **30** 1487–96
- [21] Sankar S V, Inenaga A S and Bachalo W D 1992 Trajectory dependent scattering in phase Doppler interferometry: minimizing and eliminating sizing errors *Laser Techniques and Applications in Fluid Mechanics* ed R J Adrian, D F G Durão, F Durst, M V Heitor, M Maeda and J H Whitelaw (Berlin: Springer) pp 75–89
- [22] Gréhan G, Gouesbet G, Naqwi A and Durst F 1994 Trajectory ambiguities in phase Doppler systems: study of a near forward and a near backward geometry *Particle Particle Syst. Characterization* **11** 133–44
- [23] Hardalupas Y and Taylor A M K P 1994 Phase validation criteria of size measurements for the phase Doppler technique *Exp. Fluids* **17** 253–8
- [24] Schaub S A, Alexander D R and Barton J P 1994 Theoretical analysis of the effects of particle trajectory and structural resonances on the performance of a phase Doppler particle analyser *Appl. Opt.* **33** 473–83
- [25] Sankar S V, Bachalo W D and Robart D A 1995 An adaptive intensity validation technique for minimizing trajectory dependent scattering errors in phase Doppler interferometry *4th Int. Congress on Optical Particle Sizing (Nuremberg, 1995)*
- [26] Hardalupas Y and Liu C H 1997 Implications of the Gaussian intensity distribution of laser beams on the performance of the phase Doppler technique: sizing uncertainties *Prog. Energy Combust. Sci.* **23** 41–63
- [27] Qiu H H and Hsu C T 1999 Method of phase-Doppler anemometry free from the measurement volume effect *Appl. Opt.* **38** 2737–42
- [28] Strakey P A, Talley D G, Sankar S V and Bachalo W D 2000 Phase Doppler interferometry with probe-to-droplet size ratios less than unity. I. Trajectory errors *Appl. Opt.* **39** 3875–86
- [29] Strakey P A, Talley D G, Sankar S V and Bachalo W D 2000 Phase Doppler interferometry with probe-to-droplet size ratios less than unity. II. Application of the technique *Appl. Opt.* **39** 3887–93
- [30] Haugen P, Hayes E I and von Benzon H H 1994 Size and velocity measurements of large drops in air and in a liquid-liquid two-phase flow by the phase Doppler technique *Particle Particle Syst. Characterization* **11** 63–71
- [31] Gréhan G, Gouesbet G, Naqwi A and Durst F 1993 Particle trajectory effects in phase Doppler systems: computations and experiments *Particle Particle Syst. Characterization* **10** 332–8
- [32] Fandrey C, Naqwi A, Shakal J and Zhang H 2000 A phase Doppler system for high concentration sprays *10th Int. Symp. on Applications of Laser Techniques to Fluid Mechanics (Lisbon, 2000)*

- [33] Strakey P A, Talley D G and Bachalo W D 1998 Phase Doppler measurements in dense sprays *ILASS-Americas 1998 (Sacramento, CA)* pp 291–5
- [34] Lazaro B J 1991 *Evaluation of Phase Doppler Particle Sizing in the Measurement of Optically Thick, High Number Density Sprays* UTRC91-11, United Technologies Research Center, East Hartford, CT
- [35] Van Den Moortel T, Santini R, Tadrist L and Pantaloni J 1997 Experimental study of the particle flow in a circulating fluidized bed using a phase Doppler particle analyser: a new post-processing data algorithm *Int. J. Multiphase Flow* **23** 1189–209
- [36] Widmann J F, Presser C and Leigh S D 2001 Identifying burst splitting events in phase Doppler interferometry measurements *Atomization Sprays* at press
- [37] Dodge L G, Rhodes D J and Reitz R D 1987 Drop-size measurement techniques in sprays: comparison of Malvern laser-diffraction and aerometrics phase/Doppler *Appl. Opt.* **26** 2144–54
- [38] McDonnell V G and Samuelsen G S 1988 Application of two-component phase Doppler interferometry to the measurement of particle size, mass flux and velocities in two-phase flows *22nd Symp. (Int.) on Combustion* (Combustion Institute) pp 1961–71
- [39] McDonnell V G and Samuelsen G S 1991 Gas and drop behaviour in reacting and non-reacting air-blast atomizer sprays *J. Propulsion Power* **7** 684–91
- [40] Bulzan D L, Levy Y, Aggarwal S K and Chitre S 1992 Measurements and predictions of a liquid spray from an air-assist nozzle *Atomization Sprays* **2** 445–62
- [41] Bulzan D L 1995 Structure of a swirl-stabilized combustor spray *J. Propulsion Power* **11** 1093–102
- [42] McDonnell V G and Samuelsen G S 1995 An experimental database for the computational fluid dynamics of reacting and nonreacting methanol sprays *J. Fluids Eng.* **117** 145–53
- [43] Widmann J F, Charagundla S R, Presser C and Heckert A 1999 Benchmark experimental database for multiphase combustion model input and validation: baseline case *National Institute of Standards and Technology Internal Report* 6286
- [44] Friedman J A and Renksizbulut M 1999 Investigating a methanol spray flame interacting with an annular air jet using phase Doppler interferometry and planar laser-induced fluorescence *Combust. Flame* **117** 661–84
- [45] Dodge L G and Schwalb J A 1989 Fuel spray evolution: comparison of experiment and CFD simulation of nonevaporating spray *J. Eng. Gas Turbines Power* **111** 15–23
- [46] Huber N and Sommerfeld M 1994 Characterization of the cross-sectional particle concentration distribution in pneumatic conveying systems *Powder Technol.* **79** 191–210
- [47] Sommerfeld M and Qiu H H 1998 Experimental studies of spray evaporation in turbulent flow *Int. J. Heat Fluid Flow* **19** 10–22
- [48] Berkner L, Fandrey C, Miller S, Naqwi A and Zhang H 2001 An advanced measurement system for laser Doppler and phase Doppler applications *ILASS Americas 14th Ann. Conf. on Liquid Atomization and Spray Systems (Dearborn, MI)*
- [49] Berglund R N and Liu B Y H 1973 Generation of monodisperse aerosol standards *Environ. Sci. Technol.* **7** 147–53
- [50] Widmann J F, Charagundla S R, Presser C, Yang G L and Leigh S D 2000 A correction method for spray intensity measurements obtained via phase Doppler interferometry *Aerosol Sci. Technol.* **32** 584–601
- [51] *Phase Doppler particle analyser (PDPA)—Operations Manual* 1999 (St Paul, MN: TSI)
- [52] Fleming R P 1995 Automatic sprinkler system calculations *The SFPE Handbook of Fire Protection Engineering* 2nd edn, pp 4.56–5.69
- [53] Taylor B N and Kuyatt C E Guidelines for evaluating and expressing the uncertainty of NIST measurement results *NIST Technical Note* 1297
- [54] Widmann J F 2001 Characterization of a residential fire sprinkler using phase Doppler interferometry *Atomization Sprays* at press
- [55] Widmann J F 2001 Phase Doppler interferometry measurements in water sprays produced by residential fire sprinklers *Fire Safety J.* **36** 545–67